Original Article

Nanoparticle-Mediated Delivery of Pitavastatin to Monocytes/Macrophages Inhibits Angiotensin II-Induced Abdominal Aortic Aneurysm Formation in *Apoe*−/− Mice

Shunsuke Katsuki[1], Jun-ichiro Koga[1], Tetsuya Matoba[1], Ryuta Umezu[1], Soichi Nakashiro[1], Kaku Nakano[2], Hiroyuki Tsutsui[1] and Kensuke Egashira[2, 3]

[1]The Department of Cardiovascular Medicine, Graduate School of Medical Sciences, Kyushu University, Fukuoka, Japan
[2]The Department of Cardiovascular Research, Development, and Translational Medicine, Center for Disruptive Cardiovascular Innovation, Kyushu University, Fukuoka, Japan
[3]The Department of Translational Medicine, Kyushu University Graduate School of Pharmaceutical Sciences, Fukuoka, Japan

Aim: Abdominal aortic aneurysm (AAA) is a lethal and multifactorial disease. To prevent a rupture and dissection of enlarged AAA, prophylactic surgery and stenting are currently available. There are, however, no medical therapies preventing these complications of AAA. Statin is one of the candidates, but its efficacy on AAA formation/progression remains controversial. We have previously demonstrated that nanoparticles (NPs) incorporating pitavastatin (Pitava-NPs)—clinical trials using these nanoparticles have been already conducted—suppressed progression of atherosclerosis in apolipoprotein E-deficient (*Apoe*−/−) mice. Therefore, we have tested a hypothesis that monocytes/macrophages-targeting delivery of pitavastatin prevents the progression of AAA.

Methods: Angiotensin II was intraperitoneally injected by osmotic mini-pumps to induce AAA formation in *Apoe*−/− mice. NPs consisting of poly(lactic-co-glycolic acid) were used for *in vivo* delivery of pitavastatin to monocytes/macrophages.

Results: Intravenously administered Pitava-NPs (containing 0.012 mg/kg/week pitavastatin) inhibited AAA formation accompanied with reduction of macrophage accumulation and monocyte chemoattractant protein-1 (MCP-1) expression. *Ex vivo* molecular imaging revealed that Pitava-NPs not only reduced macrophage accumulation but also attenuated matrix metalloproteinase activity in the abdominal aorta, which was underpinned by attenuated elastin degradation.

Conclusion: These results suggest that Pitava-NPs inhibit AAA formation associated with reduced macrophage accumulation and MCP-1 expression. This clinically feasible nanomedicine could be an innovative therapeutic strategy that prevents devastating complications of AAA.

Key words: Nanoparticle, Aneurysm, Inflammation, Statins, Monocyte

Introduction

Abdominal aortic aneurysm (AAA) is a frequently observed vascular disease in aged humans. In the United States, rates of ruptured aortic aneurysm range from 0.71 to 11.03 per 1000 person-years[1]. Risk of rupture dramatically increases when diameters of the enlarged aorta exceed 5.5 cm (an 85% risk of death after rupture)[2]. Prophylactic surgical intervention has been the only effective strategy for AAA rupture and aneurysm-related death. In addition, AAA increases the risk of aortic dissection that also causes sudden death. In recent years, endovascular therapies using stent grafts are increasing due to their less invasiveness. Evidence from large randomized trials reported that endovascular repair of AAA was

associated with a significantly lower operative mortality than open surgical repair[3, 4]. However, there is no long-term benefit of endovascular stent grafting in patients with AAA[5, 6]. In addition, there are limitations in stent grafting including anatomical requirements. Therefore, there remain unmet needs to develop novel medical therapies preventing AAA formation and progression.

To develop effective and innovative therapeutics, it is necessary to explore the detailed mechanisms of AAA formation. The pathobiology of AAA is characterized by multiple factors: oxidative stress, inflammation, matrix degradation, and apoptosis of medial/adventitial smooth muscle cells (SMCs)[7-9]. In terms of inflammation, accumulation of activated monocytes/macrophages promotes degradation of extracellular matrix through synthesis and release of several proteinases including matrix metalloproteinases (MMPs), which results in the expansion/rupture of AAA[10, 11]. Several animal experiments suggest that monocyte/macrophage-mediated inflammation could be a novel therapeutic target[12]. For example, siRNA-mediated gene silencing of leukocyte C-C chemokine receptor 2 (CCR2) inhibited angiotensin II-induced AAA formation[13]. D-series resolvins inhibit AAA formation through skewing macrophages toward an anti-inflammatory phenotype[14]. Clinically available drugs have also been tested in animals. HMG-CoA (3-hydroxy-3-methyl-glutaryl-CoA) reductase inhibitor has vasculoprotective and anti-inflammatory properties independent with its lipid-lowering effects[15]. In angiotensin II-infused mice, high-dose simvastatin and atorvastatin inhibit expansion of the abdominal aorta accompanied with reduction of macrophage accumulation[16, 17]. However, whether statins prevent AAA formation remains controversial[18, 19]. In humans, there are several reports about statin therapy in AAA patients. Some observational clinical studies and meta-analysis have shown that statins delayed AAA growth and mortality in patients with small AAA[20-22], but its efficacy on AAA expansion and rupture is still obscure due to lack of randomized controlled trials.

Recently, we have developed a nanotechnology-based drug delivery system (NanoDDS)[23]. We have formulated nanoparticles composed of poly(lactic-co-glycolic acid) polymers (PLGA-NPs)[24]. PLGA-NPs have the following advantages as a drug carrier: (1) deliver incorporated agents to monocytes/macrophages and sites with increased vascular permeability (e.g., inflamed sites and tumor tissues) after intravenous administration and (2) release incorporated agents after delivery to the target cells (intracellular DDS). We have previously demonstrated *in vivo* distribution of monocyte/macrophage-targeting delivery of PLGA-NPs in $Apoe^{-/-}$ mice with a high-fat diet and angiotensin II infusion[25]. Flow cytometry analysis after intravenous injection of PLGA-NPs incorporating fluorescent marker demonstrated that PLGA-NPs were predominantly delivered to monocytes in the peripheral blood and monocytes/macrophages in the vascular wall with atherosclerotic lesions. Especially, in the vascular wall, selectivity to monocytes/macrophages was over six times higher as compared with neutrophils or lymphocytes. We have developed PLGA-NPs incorporating pitavastatin (Pitava-NPs) and demonstrated their favorable effects on critical limb ischemia[26], pulmonary hypertension[27], plaque destabilization/rupture[28], and ischemia-reperfusion injury of the heart[29, 30], in which inflammation promotes their pathogenesis.

Therefore, this study aims to test the hypothesis that nanoparticle-mediated delivery of pitavastatin to monocytes/macrophages inhibits the progression of AAA. To test this hypothesis, $Apoe^{-/-}$ mice fed a high-fat diet and infused with angiotensin II were prepared[31]. To enhance the anti-inflammatory effects of pitavastatin, pitavastatin-loaded PLGA-NPs were prepared, and their efficacy on AAA was examined.

Materials and Methods

Ethics Statement

The study protocol was reviewed and approved by the Ethics Committee of Animal Experiments, Kyushu University Graduate School of Medical Sciences. This investigation conforms to the US National Institutes of Health guidelines (Guide for the Care and Use of Laboratory Animals). Blood collection and euthanasia were carried out by cervical dislocation after anesthesia with ketamine/xylazine (50 mg/kg and 1 mg/kg). Depth of anesthesia was monitored by the toe pinch reflex test.

Preparation of PLGA Nanoparticles (NPs)

A lactide/glycolide copolymer (PLGA) with an average molecular weight of 20,000 and a lactide to glycolide copolymer ratio of 75:25 (Wako Pure Chemical Industries, Osaka, Japan) was used for formulation of NPs. PLGA-NPs incorporated with fluorescein isothiocyanate (FITC; Dojindo Laboratories, Kumamoto, Japan) or pitavastatin (Kowa Pharmaceutical Co. Ltd., Tokyo, Japan) were prepared by a previously reported emulsion solvent diffusion method in purified water[32, 33]. PLGA was dissolved in a mixture of acetone and ethanol. Then, FITC or pitavastatin was added to this solution. The resultant PLGA-FITC or PLGA-pitavastatin solution was emulsified in polyvinyl alcohol solution with stirring at 400 rpm using a propeller-

type agitator with three blades (Heidon 600G; Shinto Scientific, Tokyo, Japan). After the system was agitated for 2 h under reduced pressure at 40℃, the entire suspension was centrifuged (20,000 g for 20 min at −20℃). After the supernatant was removed, purified water was added and mixed with the sediment. The wet mixture was then centrifuged again to remove the excess polyvinyl alcohol and the unencapsulated reagent that could not adsorb onto the surfaces of the NPs. After this process was repeated, the resultant dispersion was freeze-dried under the same conditions. Unencapsulated-NP (empty-NP) was also prepared. The FITC- and pitavastatin-loaded PLGA-NP contained 5.0% (w/v) FITC and 12.0% (w/v) pitavastatin, respectively. The mean particle size was analyzed by the light scattering method (Microtrack UPA150; Nikkiso, Tokyo, Japan). The average diameter of the PLGA-NP was 231 nm and 159 nm for FITC-NP and Pitava-NP, respectively. The surface charge (zeta potential) was also analyzed by Zetasizer Nano (Sysmex, Hyogo, Japan) and was found to be anionic (–16.7 mV and –4.0 mV for FITC-NP and Pitava-NP, respectively).

Experimental Animals

Male $Apoe^{-/-}$ mice (C57BL/6J genetic background) were purchased from Jackson Laboratory (Bar Harbor, ME). Animals were maintained on a 12-h light-dark cycle with free access to normal rodent chow and water.

Diet Preparation

A high-fat diet (HFD) that contained 21% fat from lard and was supplemented with 0.15% (wt/wt) pure cholesterol (Oriental yeast, Tokyo, Japan) was prepared according to the formula recommended by the American Institute of Nutrition. They contained constituents such as casein, cystine, corn starch, sucrose, cholic acid, mineral mixture, vitamin mixture, powdered cellulose, choline bitartrate, and tert-butylhydroquinone.

Experimental Protocol

At 16–18 weeks of age, mice began to receive HFD. After 4 weeks of experimental diet, all mice were infused with angiotensin II dissolved in saline at 1.9 mg/kg per day (1320 ng/kg/min) or phosphate-buffered saline (PBS) via osmotic mini-pump (Alzet, Cupertino, California, AP2004) for 4 weeks[34]. Systolic blood pressure and heart rate were measured by the tail-cuff method before and 4 weeks after angiotensin II infusion. Mice were euthanized with intraperitoneal injection of pentobarbital at 28 days after pump implantation. Blood samples were collected via

the left ventricle. Abdominal aortas were isolated and either fixed in 10% neutral buffered formalin for histological and immunohistochemical analysis or OCT compound (Sakura Finetechnical Co. Ltd., Tokyo, Japan, 4583) and stored at −80℃ for biochemical analysis.

To examine the effect of Pitava-NPs on AAA formation, animals were divided into four groups at the beginning of angiotensin II infusion: (1) no treatment group, (2) FITC-NP group (0.1 mg PLGA/200 μl PBS), (3) pitavastatin-only group (0.012 mg pitavastatin/200 μl PBS), and (4) Pitava-NP group (0.1 mg PLGA/0.012 mg pitavastatin/200 μl PBS). NPs were administered by weekly intravenous injection.

Histopathology and Analysis of AAA

Whole aorta was harvested and suprarenal lesion of the aorta was embedded in paraffin or OCT compound for immunohistochemical analysis. Sections were cut at 3 μm and 5 μm for paraffin- and OCT-embedded sections, respectively. To evaluate abdominal aorta longitudinally, three sets of serial sections obtained at 500 μm intervals were stained with elastica van Gieson (EVG). Other sections were used for immunostaining. Abdominal aortic diameter was measured at suprarenal lesion of the aorta (between celiac and right renal artery). Severity of AAA formation was determined by its macroscopic appearance of the abdominal aorta based on the following scale modified from the previously published data **(Supplementary Fig. 1A)**[35]: type I, aorta with no dilatation or thrombus; type II, dilated lumen in the suprarenal region of the aorta with no thrombus; type III, remodeled tissue in the suprarenal region that frequently contains thrombus; type IV, a pronounced bulbous of type III that contains thrombus; and type V, a form in which there are multiple aneurysms containing thrombus, some overlapping, in the suprarenal area of the aorta. Elastin degradation was determined by the EVG stain based on the following grade according to the previously published data **(Supplementary Fig. 1B)**[36]: grade 1, well-preserved elastic lamina; grade 2, one of the elastin layers was degraded; grade 3, two or more of the elastin layers were degraded; and grade 4, degradation with all elastin layers.

Immunohistochemistry

Serial arterial sections were deparaffinized, and endogenous peroxidase was blocked by incubation with 0.3% H_2O_2 in methanol for 5 min. For antigen retrieval, sections were boiled for 20 min in citrate buffer (pH=6.0). After blocking with 3% skim milk,

sections were incubated overnight at 4℃ with the respective antibodies: anti-mouse Mac-3 antibody (dilution 1:100, Santa Cruz Biotechnology Inc., Santa Cruz, California, sc-19991) and anti-mouse MCP-1 antibody (dilution 1:200, Santa Cruz Biotechnology Inc., Santa Cruz, California, sc-1785) followed by incubation with biotin-conjugated secondary antibodies. The sections were then washed and treated with avidin-peroxidase. The sections were developed using the DAB substrate kit (Wako Pure Chemical, Tokyo, Japan), and nuclei were counterstained with hematoxylin. A single observer blinded to the experimental protocol performed quantitative analysis. All images were captured with a Nikon microscope equipped with a digital camera (HC-2500) and analyzed by using Adobe Photoshop 6.0 (Adobe Systems, San Jose, California) and Scion Image 1.62 for Windows (Scion, Frederick, Maryland) software. In each case, the average value for four to five locations or sections for each animal was used for analysis.

Immunofluorescent staining was performed with frozen sections. FITC was stained with anti-FITC antibody (Abcam plc, Cambridge, UK), and nuclei were stained with VECTASHIELD Antifade Mounting Medium with DAPI (Vector Lab, Burlingame, CA). Fluorescent images were captured by confocal laser microscopy (Olympus FV1000) and analyzed by a single observer as described above.

Near-Infrared Fluorescence Molecular Imaging

Ex vivo fluorescence molecular tomography (FMT) was performed to evaluate macrophage accumulation and matrix metalloproteinase (MMP) activity as previously reported[25, 37]. We used near-infrared fluorescent nanoparticles: Aminospark 680 (Ex/Em=673/690 nm) and MMPSense 750 FAST (Ex/Em=749/775 nm) (PerkinElmer Inc., Waltham, MA, NEV10142, and NEV10168). These nanoparticles were administered via tail vein 24 h before imaging. After harvest of the heart and aorta, fluorescent signals from these nanoparticles were captured by dual-channel FMT (FMT2000, PerkinElmer, Inc.).

Statistical Analysis

All data are expressed as median±interquartile range. The statistical analysis of differences between two groups was assessed using Mann–Whitney *U*-test, and the statistical analysis of differences among more than two groups was assessed by Kruskal–Wallis test with Dunn's multiple comparison tests. Categorical valuables were assessed by Fisher's exact test. *P* value of less than 0.05 was considered to be statistically significant.

Results

Nanoparticles Were Delivered to Mac-3-Positive Macrophages in the Aortic Wall After Intravenous Administration

We have previously reported that PLGA-NPs are predominantly delivered to peripheral monocytes and macrophages in the aortic wall after intravenous injection, although part of NPs are delivered to neutrophils and lymphocytes[25]. In the vascular wall of suprarenal aorta, a predilection region of angiotensin II-induced AAA, distribution of PLGA-NPs was examined using PLGA-NPs incorporating fluorescent marker, FITC (FITC-NPs). Double immunofluorescent staining by anti-FITC and anti-Mac-3 antibody revealed that Mac-3-positive macrophages were colocalized with FITC-positive cells, suggesting that FITC-NPs were delivered to macrophages in the vascular wall **(Fig. 1)**.

Nanoparticle-Mediated Delivery of Pitavastatin to Monocytes/Macrophages Inhibits AAA Formation

Pitava-NPs containing 0.4 mg/kg pitavastatin calcium were weekly administered by tail vein for 4 weeks to examine the therapeutic effects on AAA formation. As we previously reported, Pitava-NPs have no significant effects on serum lipid profiles such as total cholesterol and triglyceride, blood pressure (systole/diastole), and heart rate after intravenous injection[28]. Pitava-NPs significantly reduced enlargement of the abdominal aorta determined as the maximum abdominal diameter at suprarenal level as compared with FITC-NPs, while pitavastatin failed to reduce the enlargement as compared with no treatment group **(Fig. 2A)**. The severity of AAA was graded based on gross findings including luminal dilatation, thrombus formation, and the shape of aortic expansion **(Supplementary Fig. 1A)**. Although pitavastatin attenuated the severity grade of AAA to some extent **(Fig. 2B)**, it was noteworthy that AAA formation, defined as >1.5 mm dilatation of the aortas[38], was markedly inhibited by Pitava-NPs. To clarify the pharmacokinetics of NP treatment, we measured the tissue concentration of pitavastatin in the liver and aorta of Pitava-NP group. The substantial tissue concentration of pitavastatin was detected in the liver **(Supplementary Table 1)**, while that of pitavastatin in the aorta was almost below the detection limit because the sample size of the aorta was too small for high-performance liquid chromatography **(Supplementary Table 2)**.
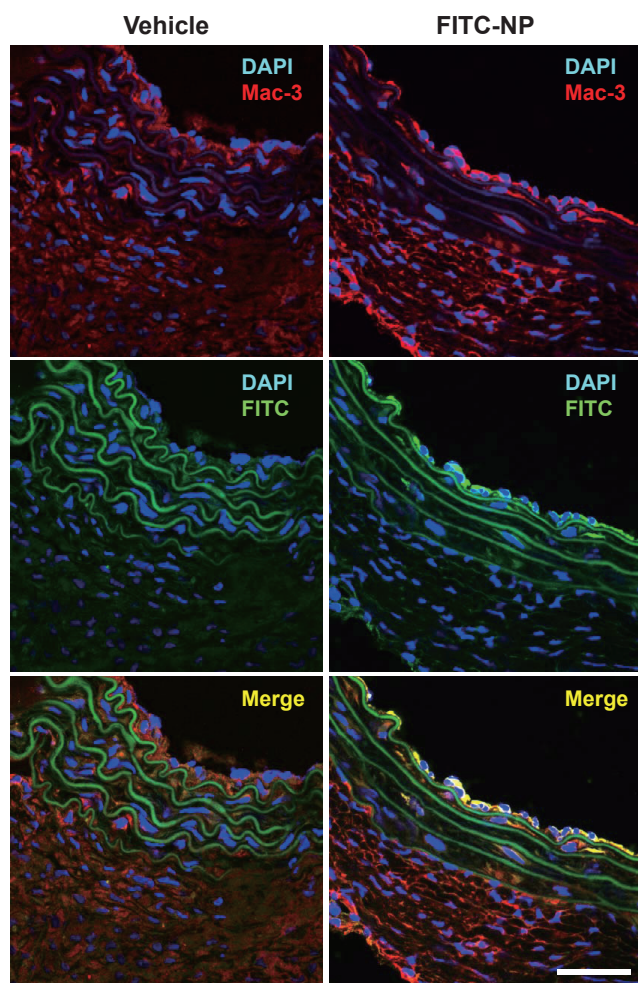
Vehicle **FITC-NP**

Fig. 1. PLGA nanoparticles are delivered to Mac-3⁺ macrophages in suprarenal aorta after intravenous administration

Nanoparticles incorporating fluorescent marker (FITC-NPs) were intravenously injected in mice after high-fat diet feeding (8 weeks) and angiotensin II infusion (4 weeks). Abdominal aorta was harvested 24 h later and distribution of nanoparticles was identified by immunofluorescent staining (FITC, Mac-3). Scale bars indicate 50 μm.

Nanoparticle-Mediated Delivery of Pitavastatin to Monocytes/Macrophages Reduces MCP-1 Expression and Macrophage Accumulation

Immunohistochemical analysis revealed accumulation of Mac-3-positive macrophages in the media and the intramural space of the enlarged aorta in FITC-NP group. MCP-1 was observed in the macrophages and medial SMCs **(Fig. 3A)**. Pitava-NPs significantly reduced the accumulation of Mac-3-positive macrophages and MCP-1 expression in total lesion of the abdominal aorta. Other investigators showed reduced mRNA levels of MCP-1 in the aorta
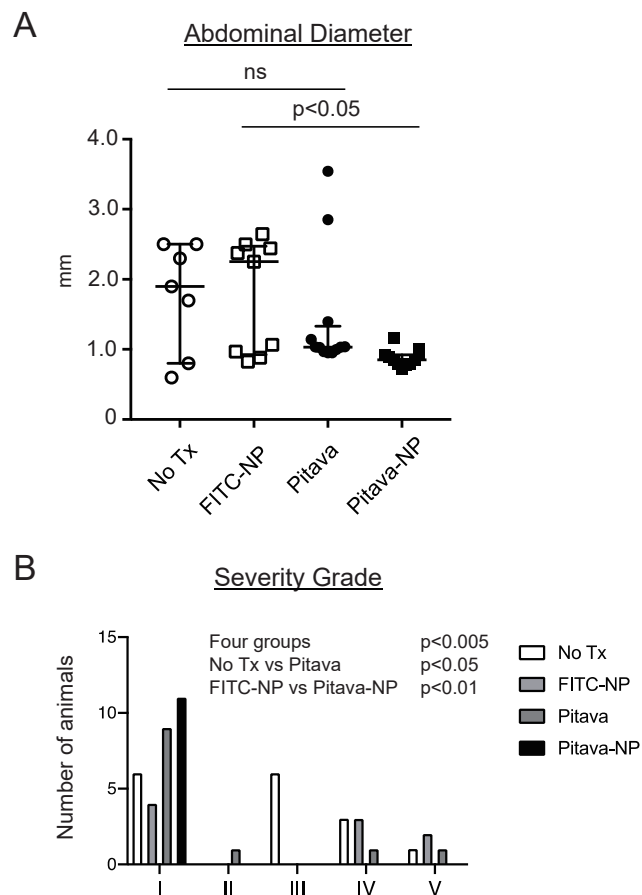

Fig. 2. Effects of Pitava-NP on expansion and severity of AAA in *Apoe⁻/⁻* mice

A, A quantitative result of abdominal diameters measured at suprarenal abdominal aorta. *N*=7, 9, 12, and 11 for No Tx, FITC-NP, Pitava, and Pitava-NP, respectively. No Tx, no treatments. The data were reported as the median ± interquartile range using by Kruskal–Wallis test with Dunn's multiple comparison tests. B, Severity grade of the abdominal aortas. *N*=16, 9, 12, and 11 for No Tx, FITC-NP, Pitava, and Pitava-NP, respectively. *P* value was calculated by Fisher's exact test.

with Pitava-NPs that we provided, which was consistent with our finding[39]. Pitava-NPs significantly reduced macrophage accumulation in non-AAA lesion, but failed to reduce MCP expression significantly because medial SMCs were still MCP-1 positive even after treatments with Pitava-NPs **(Fig. 3A)**.

Macrophage accumulation was also observed *ex vivo* using a near-infrared fluorescence (NIRF) molecular imaging. Nanoparticles consisting of an iron oxide core were intravenously injected to visualize macrophage accumulation in the aneurysmal lesion. Fluorescent signals emitted by accumulating probes were observed in enlarged abdominal aorta, which was significantly attenuated by Pitava-NPs **(Fig. 3B).**
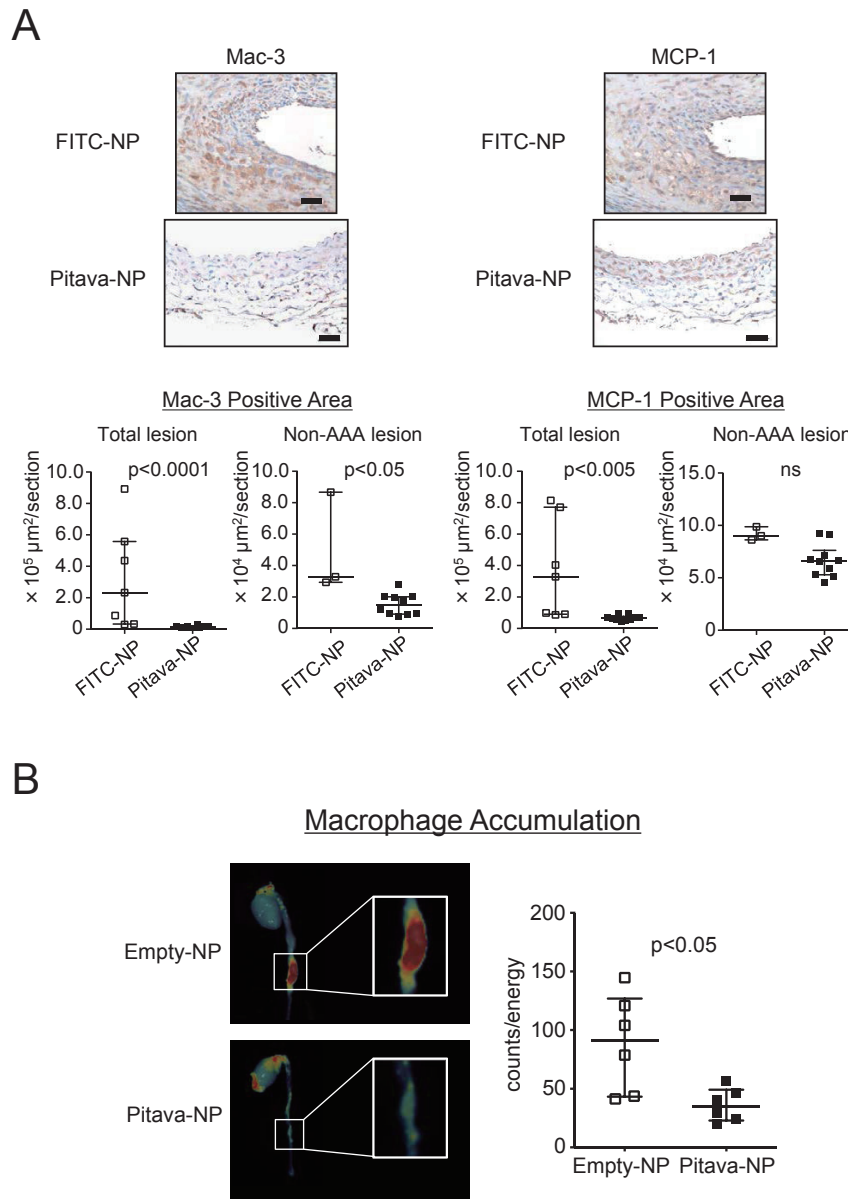
Fig. 3. Nanoparticle-mediated delivery of pitavastatin to monocytes/macrophages suppresses macrophage accumulation to the aneurysmal aorta

A, Left panels: photomicrographs of suprarenal abdominal aorta stained with anti-Mac-3 antibody. The scale bar indicates 50 μm. Right panels: photomicrographs of suprarenal abdominal aorta stained with anti-MCP-1 antibody. Lower graphs indicate the results of quantitative analysis in total and non-AAA lesion. $N = 7$ and 10 for total lesion and $N = 3$ and 10 for non-AAA lesion, respectively. The data are reported as the median ± interquartile range using Mann–Whitney *U*-test. B, *Ex vivo*, near-infrared fluorescent imaging showing macrophage accumulation. Fluorescent nanoparticles with iron oxide core were injected by tail vein 24 h before imaging. Right graph shows quantitative data of fluorescent signal counts. $N = 6$. The data were reported as the median ± interquartile range using Mann–Whitney *U*-test.

Pitava-NP Inhibits Elastin Degradation and MMP Activities in the Aneurysmal Aortic Lesions

Proteinases including matrix metalloproteinases (MMPs), cathepsins, and elastases degrade extracellular matrix and promote enlargement of the aorta[40-42]. Especially, loss of elastin causes enlargement and rupture of the aneurysmal aorta[43]. Hence, we focused on elastin degradation and analyzed histopathologic features of abdominal aortic lesions. In FITC-NP group, intramural hematoma was observed adjacent to the disrupted elastin layers. On the other hand, elastin layers were well-preserved in Pitava-NP group. Elastin degradation score tended to reduce in Pitava-NP group **(Fig. 4A and Supplementary**
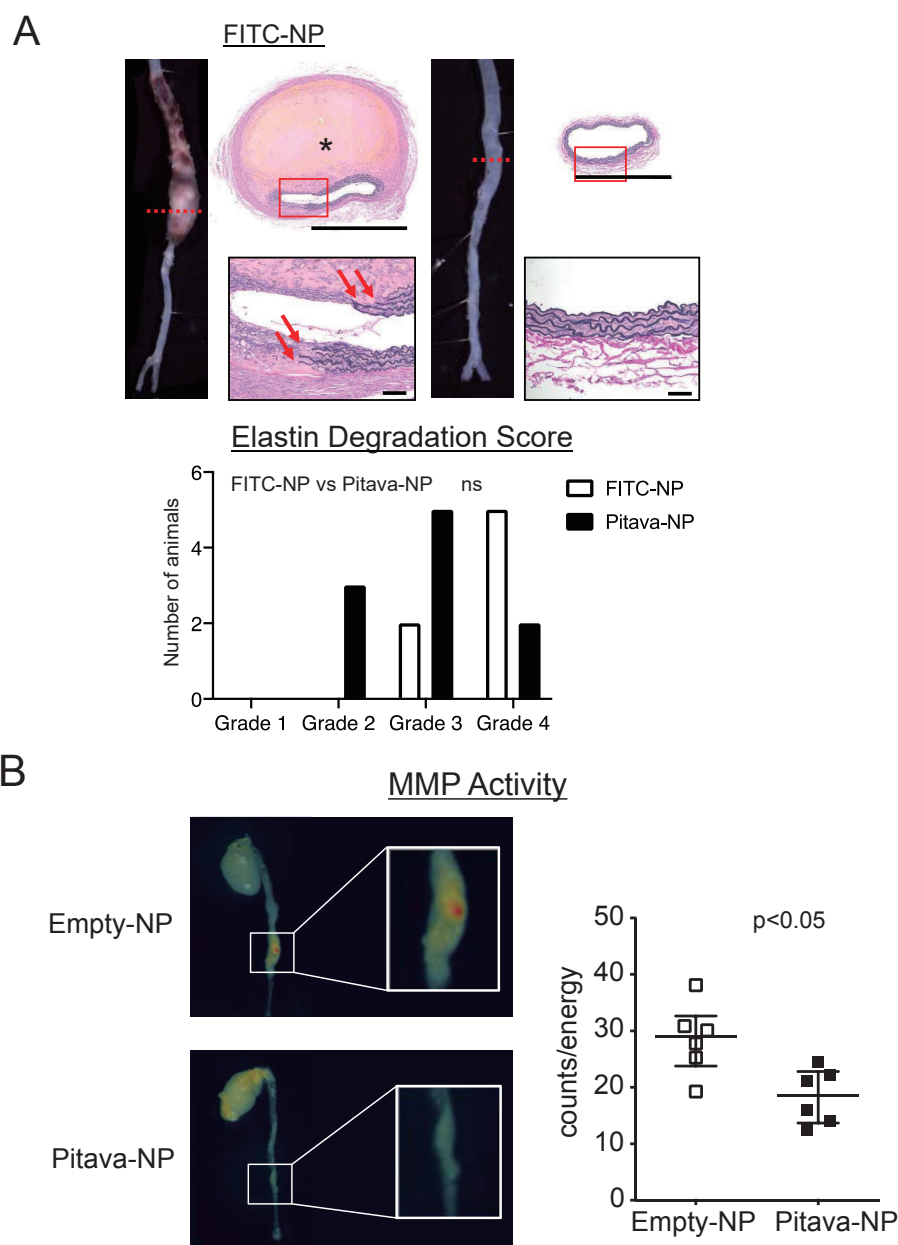
Fig. 4. Pitava-NPs inhibit elastin degradation and MMP activities in the aneurysmal aorta

A, Upper panels: photographs and photomicrographs of suprarenal abdominal aortas. Sections were stained with elastica van Gieson (EVG) solution. Asterisk shows intramural hematoma. The scale bar indicates 1 mm and 50 μm for magnified image. Lower panel: elastin degradation score of the abdominal aortas. $N=7$ and 10 for FITC-NP and Pitava-NP, respectively. The data were assessed by Fisher's exact test. B, *Ex vivo*, near-infrared fluorescent imaging showing MMP activities. Nanoparticles with quenched and MMP-activatable fluorescence were injected by tail vein 24 h before imaging. Right graph shows quantitative data of fluorescent signal counts. $N=6$. The data were reported as the median ± interquartile range using Mann–Whitney U-test.

Fig. 1B).

We then evaluated MMP activities in the aorta by NIRF imaging using MMP-activatable probe named MMPSense. MMP-12 is known as macrophage elastase and both MMP-2 and MMP-9 have elastolytic properties during the development of AAA[44, 45]. MMPSense emits near-infrared signal when cleaved by MMPs including MMP-2, MMP-9, and MMP-12. *Ex vivo* fluorescent molecular tomography demonstrated increased MMP activity in the aneurysmal aorta. Pitava-NP significantly attenuated MMP activity in the aorta **(Fig. 4B)**.

Discussion

In this study, we demonstrated that NP-mediated delivery of pitavastatin to monocytes/macrophages inhibits angiotensin II-induced AAA formation in hyperlipidemic mice. The following are the major findings of this study: (1) PLGA-NPs were delivered to macrophages in the vascular wall of suprarenal aorta after intravenous injection; (2) Pitava-NP markedly inhibited AAA formation; (3) Pitava-NP reduced macrophage accumulation and MCP-1 expression in the vascular wall; and (4) Pitava-NP tended to inhibit elastin degradation, accompanied with attenuated MMP activities.

Patients with AAA diameter over 50 mm undergo surgical repair/replacement of the enlarged aorta to prevent rupture of AAA[46]. In recent years, less invasive endovascular surgery has become a common procedure, but a certain number of patients are not indicated to surgeries due to anatomical reasons or systemic conditions. Furthermore, there are no effective therapeutic options in patients with AAA diameter between 30 and 50 mm. The efficacies of currently available medicine (e.g., statins, β-blocker, ACE inhibitor/ARB, and other antihypertensive drugs) on AAA progression and its complications remain controversial[22, 47]. In experimental animals, various medical agents, including MMP inhibitor, JNK inhibitor, and NF-κB decoy, are tested as therapeutics for AAA, and their efficacies are reported[48, 49], but these agents have to overcome many steps including toxicity tests before the clinical application, which needs a significant amount of time and cost.

Statins exert their therapeutic effects by several mechanisms including anti-inflammatory and anti-oxidative effects, besides their lipid-lowering effects. Serum total cholesterol concentration itself is reported not to be associated with the progression of AAA[48]. However, the therapeutic effects of statins remain controversial and are not consistent in both animal and clinical studies. Animal studies have suggested a possibility that each statin has different effects on the pathobiology of AAA[16, 17, 50], which may cause inconsistent results of clinical studies. In addition, pharmacokinetics of each statin is different, and drug concentration in target tissues might not be sufficient in several clinical trials.

Considering these possibilities, we used a pitavastatin-loaded polymeric nanoparticle as a therapeutic agent for AAA in this study. We adopted pitavastatin as loaded statin for this nanoparticle because this compound demonstrates the most potent inhibitory effects on HMG-CoA reductase activity among commercially available statins[51].

Nanoparticle-based drug delivery systems can improve the pharmacokinetics of pitavastatin by promoting delivery to phagocytic monocytes/macrophages and escaping delivery to non-targeted tissues[24, 25, 27, 28, 50]. We have already demonstrated *in vivo* distribution of the intravenously injected PLGA-NP in hyperlipidemic and angiotensin II-infused $Apoe^{-/-}$ mice[25]. In the study, we have clarified that FITC-NPs were delivered to monocytes, neutrophils, and part of lymphocytes in the peripheral blood by intravenous injection and retained longer than FITC solution. FITC-NPs were predominantly delivered to circulating monocytes and macrophages in the aorta with atherosclerotic plaques. While FITC signal reaches the peak 2 h after injection of FITC-NPs and is also detected reduced by half 2 days later in the blood, FITC signal reaches the peak 2 days after injection and remained in the vascular wall over 7 days after injection. Based on these results, we intravenously administered Pitava-NPs once a week. Weekly intravenous treatment with Pitava-NPs inhibited AAA formation associated with reduced macrophage infiltration without affecting serum cholesterol and triglyceride levels.

To elucidate the mechanisms underlying the therapeutic effects of Pitava-NP in AAA, we examined macrophage-mediated inflammation in the abdominal aorta. Pitava-NP significantly reduced macrophage accumulation in the media and intramural space of the abdominal aorta. MCP-1 expression of the abdominal aorta was colocalized with lesional macrophages and medial SMCs in the control group. We have already reported that Pitava-NP reduced MCP-1 gene expression and MCP-1-induced chemotaxis using monocyte/macrophage-like cells[28]. All of these data suggested that accumulating macrophages express MCP-1 and then the MCP-1 might accelerate monocyte infiltration to the vascular wall leading to a vicious cycle of macrophage-mediated inflammation, which was ameliorated by Pitava-NPs. We analyzed macrophage accumulation and MCP-1 expression not only in total lesion but also in non-AAA lesion, because it is more reasonable to exclude AAA lesion to provide insights into understanding mechanisms. Although Pitava-NP failed to abrogate MCP-1 expression in non-AAA lesion since MCP-1 was still observed in the medial SMCs even in Pitava-NP group, reduced MCP-1-induced chemotaxis by Pitava-NP might involve the mechanism of the reduced macrophage infiltration to the arterial wall even in the presence of MCP-1. Hence, NP-mediated inhibition of MCP-1 could be a mechanism underlying these therapeutic effects of

Pitava-NP on AAA formation. We and other investigators reported that CCR2 on expressed monocytes is critical in angiotensin II-induced AAA formation[13, 34]. These studies suggested that monocyte/macrophage MCP-1/CCR2 signaling might be a favorable therapeutic target to prevent AAA formation.

This study has several limitations. First, we adopted the protocol of weekly intravenous administration of NPs only at the indicated dose because the protocol also had noteworthy therapeutic effects on atherosclerotic plaque destabilization and rupture[28]. Further studies are needed to clarify whether more therapeutic effects may be obtained by optimization of the injection dose. Also, we could not clarify the pharmacokinetics of NP treatment in this study because the sample size of the murine aorta was too small for high-performance liquid chromatography. We need to measure tissue concentration of pitavastatin in the abdominal aorta for *in vivo* pharmacokinetics using larger animals. Second, we adopted pitavastatin as a loaded drug of NPs at this time due to its potent inhibitory effects of HMG-CoA reductase activity and clinical feasibility of Pitava-NP that we have developed. Previous studies suggest that distinct statins can affect different signaling pathways to prevent AAA formation[48]. It remains to be elucidated in the future whether the beneficial effects of Pitava-NP on the prevention of AAA formation are drug class effects of statins by using nanoparticles loaded with other statins than pitavastatin.

In conclusion, NP-mediated delivery of pitavastatin inhibits angiotensin II-induced AAA formation by attenuating macrophage accumulation and matrix degradation. The pitavastatin-loaded nanoparticle used in this study has been already tested in phase I and IIa clinical trials (clinical trial registry identifier: UMIN000014940 and UMIN000019189) in healthy subjects and in patients with critical limb ischemia. These clinical trials have been completed without any serious adverse side effects, and the nanoparticle is going to be tested in large-scale clinical trials. To the best of our knowledge, this is the first study to demonstrate clinically feasible nanoparticle-mediated therapy for the prevention of AAA formation. Finally, this novel modality can be developed as a next-generation prophylactic strategy for atherosclerotic cardiovascular diseases.

Acknowledgments

Funding

Conflict of Interest

This work was supported by research grant from Kowa Life Science Foundation (to S.K. and J.K.). K.N. is currently employed by Kowa Company, Ltd., but he had no conflict of interest when this work was done. The remaining authors report no conflicts of interest.

References

1) Benjamin EJ, Blaha MJ, Chiuve SE, Cushman M, Das SR, Deo R, de Ferranti SD, Floyd J, Fornage M, Gillespie C, Isasi CR, Jimenez MC, Jordan LC, Judd SE, Lackland D, Lichtman JH, Lisabeth L, Liu S, Longenecker CT, Mackey RH, Matsushita K, Mozaffarian D, Mussolino ME, Nasir K, Neumar RW, Palaniappan L, Pandey DK, Thiagarajan RR, Reeves MJ, Ritchey M, Rodriguez CJ, Roth GA, Rosamond WD, Sasson C, Towfighi A, Tsao CW, Turner MB, Virani SS, Voeks JH, Willey JZ, Wilkins JT, Wu JH, Alger HM, Wong SS, Muntner P, American Heart Association Statistics C and Stroke Statistics S. Heart Disease and Stroke Statistics-2017 Update: A Report From the American Heart Association. Circulation, 2017; 135: e146-e603

2) Powell JT, Brady AR, Brown LC, Forbes JF, Fowkes FGR, Greenhalgh RM, Ruckley CV, Thompson SG and Participants USAT. Mortality results for randomised controlled trial of early elective surgery or ultrasonographic surveillance for small abdominal aortic aneurysms. Lancet, 1998; 352: 1649-1655

3) De Bruin JL, Baas AF, Buth J, Prinssen M, Verhoeven ELG, Cuypers PWM, van Sambeek MRHM, Balm R, Grobbee DE, Blankensteijn JD and Grp DS. Long-Term Outcome of Open or Endovascular Repair of Abdominal Aortic Aneurysm. New Engl J Med, 2010; 362: 1881-1889

4) Greenhalgh RM, Brown LC, Powell JT, Thompson SG and Epstein D. Endovascular repair of aortic aneurysm in patients physically ineligible for open repair. N Engl J Med, 2010; 362: 1872-1880

5) Lederle FA, Freischlag JA, Kyriakides TC, Matsumura JS, Padberg FT, Kohler TR, Kougias P, Jean-Claude JM, Cikrit DF, Swanson KM and Study OVAC. Long-Term Comparison of Endovascular and Open Repair of Abdominal Aortic Aneurysm. New Engl J Med, 2012; 367: 1988-1997

6) Kent KC. Clinical practice. Abdominal aortic aneurysms. N Engl J Med, 2014; 371: 2101-2108

7) Lu H and Daugherty A. Aortic Aneurysms. Arterioscl Throm Vas, 2017; 37: E59-E65

8) McCormick ML, Gavrila D and Weintraub NL. Role of oxidative stress in the pathogenesis of abdominal aortic aneurysms. Arterioscl Throm Vas, 2007; 27: 461-469

9) Weintraub NL. Understanding Abdominal Aortic Aneurysm. New Engl J Med, 2009; 361: 1114-1116

10) Shimizu K, Mitchell RN and Libby P. Inflammation and cellular immune responses in abdominal aortic aneurysms. Arterioscl Throm Vas, 2006; 26: 987-994

11) Manning MW, Cassis LA and Daugherty A. Differential effects of doxycycline, a broad-spectrum matrix metalloproteinase inhibitor, on angiotensin II-induced atherosclerosis and abdominal aortic aneurysms. Arterioscl Throm Vas, 2003; 23: 483-488

12) Raffort J, Lareyre F, Clement M, Hassen-Khodja R, Chinetti G and Mallat Z. Monocytes and macrophages in abdominal aortic aneurysm. Nat Rev Cardiol, 2017; 14: 457-471

13) de Waard V, Bot I, de Jager SC, Talib S, Egashira K, de Vries MR, Quax PH, Biessen EA and van Berkel TJ. Systemic MCP1/CCR2 blockade and leukocyte specific MCP1/CCR2 inhibition affect aortic aneurysm formation differently. Atherosclerosis, 2010; 211: 84-89

14) Pope NH, Salmon M, Davis JP, Chatterjee A, Su G, Conte MS, Ailawadi G and Upchurch GR. D-series resolvins inhibit murine abdominal aortic aneurysm formation and increase M2 macrophage polarization. Faseb J, 2016; 30: 4192-4201

15) Takemoto M and Liao JK. Pleiotropic effects of 3-hydroxy-3-methylglutaryl coenzyme a reductase inhibitors. Arterioscler Thromb Vasc Bio, 2001; 21: 1712-1719

16) Zhang YL, Naggar JC, Welzig CM, Beasley D, Moulton KS, Park HJ and Galper JB. Simvastatin Inhibits Angiotensin II-Induced Abdominal Aortic Aneurysm Formation in Apolipoprotein E-Knockout Mice Possible Role of ERK. Arterioscl Throm Vas, 2009; 29: 1764-U110

17) Li YY, Lu GS, Sun DT, Zuo HJ, Wang DW and Yan JT. Inhibition of endoplasmic reticulum stress signaling pathway: A new mechanism of statins to suppress the development of abdominal aortic aneurysm. Plos One, 2017; 12

18) Golledge J, Cullen B, Moran C and Rush C. Efficacy of Simvastatin in Reducing Aortic Dilatation in Mouse Models of Abdominal Aortic Aneurysm. Cardiovasc Drug Ther, 2010; 24: 373-378

19) Wang JA, Chen WA, Wang Y, Zhang S, Bi H, Hong B, Luo Y, Daugherty A and Xie X. Statins exert differential effects on angiotensin II-induced atherosclerosis, but no benefit for abdominal aortic aneurysms. Atherosclerosis, 2011; 217: 90-96

20) Sukhija R, Aronow WS, Sandhu R, Kakar P and Babu S. Mortality and size of abdominal aortic aneurysm at long-term follow-up of patients not treated surgically and treated with and without statins. Am J Cardiol, 2006; 97: 279-280

21) Schouten O, van Laanen JH, Boersma E, Vidakovic R, Feringa HH, Dunkelgrun M, Bax JJ, Koning J, van Urk H and Poldermans D. Statins are associated with a reduced infrarenal abdominal aortic aneurysm growth. Eur J Vasc Endovasc Surg, 2006; 32: 21-26

22) Takagi H, Matsui M and Umemoto T. A meta-analysis of clinical studies of statins for prevention of abdominal aortic aneurysm expansion. J Vasc Surg, 2010; 52: 1675-1681

23) Katsuki S, Matoba T, Koga JI, Nakano K and Egashira K. Anti-inflammatory Nanomedicine for Cardiovascular Disease. Front Cardiovasc Med, 2017; 4: 87

24) Koga J, Matoba T and Egashira K. Anti-inflammatory Nanoparticle for Prevention of Atherosclerotic Vascular Diseases. J Atheroscler Thromb, 2016; 23: 757-765

25) Nakashiro S, Matoba T, Umezu R, Koga J, Tokutome M, Katsuki S, Nakano K, Sunagawa K and Egashira K. Pioglitazone-Incorporated Nanoparticles Prevent Plaque Destabilization and Rupture by Regulating Monocyte/Macrophage Differentiation in ApoE(-/-) Mice. Arterioscl Throm Vas, 2016; 36: 491-500

26) Kubo M, Egashira K, Inoue T, Koga J, Oda S, Chen L, Nakano K, Matoba T, Kawashima Y, Hara K, Tsujimoto H, Sueishi K, Tominaga R and Sunagawa K. Therapeutic Neovascularization by Nanotechnology-Mediated Cell-Selective Delivery of Pitavastatin Into the Vascular Endothelium. Arterioscl Throm Vas, 2009; 29: 796-U47

27) Chen L, Nakano K, Kimura S, Matoba T, Iwata E, Miyagawa M, Tsujimoto H, Nagaoka K, Kishimoto J, Sunagawa K and Egashira K. Nanoparticle-mediated delivery of pitavastatin into lungs ameliorates the development and induces regression of monocrotaline-induced pulmonary artery hypertension. Hypertension, 2011; 57: 343-350

28) Katsuki S, Matoba T, Nakashiro S, Sato K, Koga J, Nakano K, Nakano Y, Egusa S, Sunagawa K and Egashira K. Nanoparticle-Mediated Delivery of Pitavastatin Inhibits Atherosclerotic Plaque Destabilization/Rupture in Mice by Regulating the Recruitment of Inflammatory Monocytes. Circulation, 2014; 129: 896-906

29) Nagaoka K, Matoba T, Mao YJ, Nakano Y, Ikeda G, Egusa S, Tokutome M, Nagahama R, Nakano K, Sunagawa K and Egashira K. A New Therapeutic Modality for Acute Myocardial Infarction: Nanoparticle-Mediated Delivery of Pitavastatin Induces Cardioprotection from Ischemia-Reperfusion Injury via Activation of PI3K/Akt Pathway and Anti-Inflammation in a Rat Model. Plos One, 2015; 10

30) Ichimura K, Matoba T, Nakano K, Tokutome M, Honda K, Koga J and Egashira K. A Translational Study of a New Therapeutic Approach for Acute Myocardial Infarction: Nanoparticle-Mediated Delivery of Pitavastatin into Reperfused Myocardium Reduces Ischemia-Reperfusion Injury in a Preclinical Porcine Model. Plos One, 2016; 11

31) Daugherty A, Manning MW and Cassis LA. Angiotensin II promotes atherosclerotic lesions and aneurysms in apolipoprotein E-deficient mice. J Clin Invest, 2000; 105: 1605-1612

32) Murakami H, Kobayashi M, Takeuchi H and Kawashima Y. Preparation of poly(DL-lactide-co-glycolide) nanoparticles by modified spontaneous emulsification solvent diffusion method. Int J Pharm, 1999; 187: 143-

152

33) Kawashima Y, Yamamoto H, Takeuchi H, Hino T and Niwa T. Properties of a peptide containing DL-lactide/glycolide copolymer nanospheres prepared by novel emulsion solvent diffusion methods. Eur J Pharm Biopharm, 1998; 45: 41-48

34) Ishibashi M, Egashira K, Zhao Q, Hiasa K, Ohtani K, Ihara Y, Charo IF, Kura S, Tsuzuki T, Takeshita A and Sunagawa K. Bone marrow-derived monocyte chemoattractant protein-1 receptor CCR2 is critical in angiotensin II-induced acceleration of atherosclerosis and aneurysm formation in hypercholesterolemic mice. Arterioscler Thromb Vasc Biol, 2004; 24: e174-178

35) Daugherty A, Manning MW and Cassis LA. Antagonism of AT2 receptors augments Angiotensin II-induced abdominal aortic aneurysms and atherosclerosis. Brit J Pharmacol, 2001; 134: 865-870

36) Satoh K, Nigro P, Matoba T, O'Dell MR, Cui Z, Shi X, Mohan A, Yan C, Abe J, Illig KA and Berk BC. Cyclophilin A enhances vascular oxidative stress and the development of angiotensin II-induced aortic aneurysms. Nat Med, 2009; 15: 649-656

37) Koga J, Nakano T, Dahlman JE, Figueiredo JL, Zhang HM, Decano J, Khan OF, Niida T, Iwata H, Aster JC, Yagita H, Anderson DG, Ozaki CK and Aikawa M. Macrophage Notch Ligand Delta-Like 4 Promotes Vein Graft Lesion Development Implications for the Treatment of Vein Graft Failure. Arterioscl Throm Vas, 2015; 35: 2343-2353

38) Gitlin JM, Trivedi DB, Langenbach R and Loftin CD. Genetic deficiency of cyclooxygenase-2 attenuates abdominal aortic aneurysm formation in mice. Cardiovasc Res, 2007; 73: 227-236

39) Sun Y, Chen L, Zhao S, Shi L, Li H, Tian W and Qi G. Effects of nanoparticle-mediated delivery of pitavastatin on atherosclerotic plaques in ApoE-knockout mice and THP-1-derived macrophages. Exp Ther Med, 2020; 19: 3787-3797

40) Sun JS, Sukhova GK, Zhang J, Chen H, Sjoberg S, Libby P, Xia MC, Xiong N, Gelb BD and Shi GP. Cathepsin K Deficiency Reduces Elastase Perfusion-Induced Abdominal Aortic Aneurysms in Mice. Arterioscl Throm Vas, 2012; 32: 15-U68

41) Nosoudi N, Nahar-Gohad P, Sinha A, Chowdhury A, Gerard P, Carsten CG, Gray BH and Vyavahare NR. Prevention of Abdominal Aortic Aneurysm Progression by Targeted Inhibition of Matrix Metalloproteinase Activity With Batimastat-Loaded Nanoparticles. Circ Res, 2015; 117: E80-E89

42) Busuttil RW, Rinderbriecht H, Flesher A and Carmack C. Elastase Activity - the Role of Elastase in Aortic-Aneurysm Formation. J Surg Res, 1982; 32: 214-217

43) Hellenthal FA, Buurman WA, Wodzig WK and Schurink GW. Biomarkers of AAA progression. Part 1: extracellular matrix degeneration. Nat Rev Cardiol, 2009; 6: 464-474

44) Pyo R, Lee JK, Shipley JM, Curci JA, Mao D, Ziporin SJ, Ennis TL, Shapiro SD, Senior RM and Thompson RW. Targeted gene disruption of matrix metalloproteinase-9 (gelatinase B) suppresses development of experimental abdominal aortic aneurysms. J Clin Invest, 2000; 105: 1641-1649

45) Senior RM, Griffin GL, Fliszar CJ, Shapiro SD, Goldberg GI and Welgus HG. Human 92- and 72-kilodalton type IV collagenases are elastases. J Biol Chem, 1991; 266: 7870-7875

46) Baxter BT, Terrin MC and Dalman RL. Medical management of small abdominal aortic aneurysms. Circulation, 2008; 117: 1883-1889

47) Lederle FA, Noorbaloochi S, Nugent S, Taylor BC, Grill JP, Kohler TR and Cole L. Multicentre study of abdominal aortic aneurysm measurement and enlargement. Br J Surg, 2015; 102: 1480-1487

48) Miyake T and Morishita R. Pharmacological treatment of abdominal aortic aneurysm. Cardiovasc Res, 2009; 83: 436-443

49) Yoshimura K, Aoki H, Ikeda Y, Fujii K, Akiyama N, Furutani A, Hoshii Y, Tanaka N, Ricci R, Ishihara T, Esato K, Hamano K and Matsuzaki M. Regression of abdominal aortic aneurysm by inhibition of c-Jun N-terminal kinase. Nat Med, 2005; 11: 1330-1338

50) Nagashima H, Aoka Y, Sakomura Y, Sakuta A, Aomi S, Ishizuka N, Hagiwara N, Kawana M and Kasanuki H. A 3-hydroxy-3-methylglutaryl coenzyme A reductase inhibitor, cerivastatin, suppresses production of matrix metalloproteinase-9 in human abdominal aortic aneurysm wall. J Vasc Surg, 2002; 36: 158-163

51) Aoki T, Nishimura H, Nakagawa S, Kojima J, Suzuki H, Tamaki T, Wada Y, Yokoo N, Sato F, Kimata H, Kitahara M, Toyoda K, Sakashita M and Saito Y. Pharmacological profile of a novel synthetic inhibitor of 3-hydroxy-3-methylglutaryl-coenzyme A reductase. Arzneimittelforschung, 1997; 47: 904-909

Supplementary Materials and Methods

Ethics Statement

The study protocol was reviewed and approved by the Committee on the Ethics of Animal Experiments, Kyushu University Graduate School of Medical Sciences. This investigation conforms the US National Institutes of Health guidelines (Guide for the Care and Use of Laboratory Animals). Blood collection and euthanasia were carried out by cervical dislocation after anesthesia with ketamine/xylazine (50 mg/kg and 1 mg/kg). Depth of anesthesia was monitored by the toe pinch reflex test.

Preparation of PLGA Nanoparticles (NPs)

A lactide/glycolide copolymer (PLGA) with an average molecular weight of 20,000 and a lactide to glycolide copolymer ratio of 75:25 (Wako Pure Chemical Industries, Osaka, Japan) was used for formulation of NPs. PLGA-NPs incorporated with fluorescein isothiocyanate (FITC; Dojindo laboratories, Kumamoto, Japan) or pitavastatin (Kowa Pharmaceutical Co Ltd, Tokyo, Japan) was prepared by a previously reported emulsion solvent diffusion method in purified water[1, 2]. PLGA was dissolved in a mixture of acetone and ethanol. Then, FITC or pitavastatin was added to this solution. The resultant PLGA-FITC or PLGA-pitavastatin solution was emulsified in polyvinyl alcohol solution with stirring at 400 rpm using a propeller-type agitator with 3 blades (Heidon 600G; Shinto Scientific, Tokyo, Japan). After the system was agitated for 2 hours under reduced pressure at 40℃, the entire suspension was centrifuged (20,000 g for 20 minutes at −20℃). After the supernatant was removed, purified water was added and mixed with the sediment. The wet mixture was then centrifuged again to remove the excess polyvinyl alcohol and the unencapsulated reagent that could not adsorb onto the surfaces of the NPs. After this process was repeated, the resultant dispersion was freeze-dried under the same conditions. Unencapsulated-NP (empty-NP) was also prepared. The FITC- and pitavastatin-loaded PLGA-NP contained 5.0% (w/v) FITC and 12.0% (w/v) pitavastatin, respectively. The mean particle size was analyzed by the light scattering method (Microtrack UPA150; Nikkiso, Tokyo, Japan). The average diameter of the PLGA-NP was 231 nm and 159 nm for FITC-NP and Pitava-NP, respectively. The surface charge (zeta potential) was also analyzed by Zetasizer Nano (Sysmex, Hyogo, Japan) and was found to be anionic (-16.7 mV and -4.0 mV for FITC-NP and Pitava-NP, respectively).

Experimental Animals

Male apolipoorotein E-deficient ($Apoe^{-/-}$) mice (C57BL/6J genetic background) were purchased from Jackson Laboratory (BarHarbor, ME). Animals were maintained on a 12-h light-dark cycle with free access to normal rodent chow and water.

Diet Preparation

A high-fat diet (HFD) that contained 21% fat from lard and was supplemented with 0.15% (wt/wt) pure cholesterol (Oriental yeast, Tokyo, Japan) were prepared according to the formula recommended by the American Institute of Nutrition. They contained the following constituents: casein, cystine, corn starch, sucrose, cholic acid, mineral mixture, vitamin mixture, powdered cellulose, choline bitartrate, and tert-butylhydroquinone.

Experimental Protocol

The study protocol was reviewed and approved by the Committee on the Ethics of Animal Experiments, Kyushu University Graduate School of Medical Sciences. At 16-18 weeks of age, mice began to receive HFD. After 4 weeks of experimental diet, all mice were infused with angiotensin II dissolved in saline at 1.9 mg/kg per day (1320 ng/kg/min) or phosphate buffered saline (PBS) via osmotic mini-pump (Alzet, Cupertino, California, AP2004) for 4 weeks[3, 4]. Systolic blood pressure and heart rate were measured by the tail-cuff method before and 4 weeks after angiotensin II infusion. Mice were euthanized with intraperitoneal injection of pentobarbital at day 28 of angiotensin II infusion for analysis. Blood samples were collected via the left ventricle. Abdominal aortas were isolated and either fixed in 10 % buffered formalin for histological and immunohistochemical analysis or OCT compound (Sakura Finetechnical Co Ltd, Tokyo, Japan, 4583), and stored at −80℃ for biochemical analysis.

To examine the effect of nanoparticle-mediated monocyte-selective delivery of pitavastatin on AAA formation, animals were divided into 4 groups at the beginning of angiotensin II infusion: (1) no treatment group; (2) FITC-incorporated NP group (0.1 mg PLGA/ 200 μl PBS); (3) Pitvastatin-only group (0.012 mg Pitavastatin/ 200 μl PBS); and (4) Pitavastatin-incorporated NP group (0.1 mg PLGA/ 0.012 mg Pitavastatin/ 200 μl PBS). NPs were administered by weekly intravenous injection. The dose of pitavastatin-NP used in this study was selected because the effectiveness was confirmed in hind limb ischemia model reported in a prior study[5].

Histopathology and Analysis of AAA

Whole aorta was harvested and suprarenal lesion of the aorta was embedded in paraffin or OCT compound for immunohistochemical analysis. Sections were cut at 3 μm for paraffin-embedded sections and 5 μm for OCT-embedded sections. To evaluate abdominal aorta longitudinally, three sets of serial sections obtained at 500 μm intervals were stained with elastica van Gieson (EVG). Other sections were used for immunostaining. Abdominal aortic diameter was measured at suprarenal lesion of aorta (between celiac and right renal artery). Severity of AAA formation was determined by its macroscopic appearance of abdominal aorta based on the following scale modified from the previously published data (Supplementary figure IA)[6]: Type I, aorta with no dilatation or thrombus. Type II, dilated lumen in the suprarenal region of the aorta with no thrombus. Type III, remodeled tissue in the suprarenal region that frequently contains thrombus. Type IV, a pronounced bulbous of type III that contains thrombus. Type V, a form in which there are multiple aneurysms containing thrombus, some overlapping, in the suprarenal area of the aorta. Elastin degradation was determined by the EVG stain based on the following grade according to the previously published data (Supplementary figure IB)[7]: Grade 1, well preserved elastic lamina. Grade 2, one of elastin layers was degraded. Grade 3, two or more of elastin layers were degradated. Grade 4, degradation with all elastin layers.

Immunohistochemistry

Serial arterial sections were deparaffinized, and endogenous peroxidase was blocked by incubation with 0.3 % H_2O_2 in methanol for 5 minutes. For antigen retrieval, sections were boiled for 20 minutes in citrate buffer (pH=6.0). After blocking with 3% skim milk, sections were incubated overnight at 4℃ with the respective antibodies: anti-mouse macrophage antibody (Mac-3; dilution 1:100, Santa Cruz Biotechnology Inc, Santa Cruz, California, sc-19991), and anti-mouse MCP-1 antibody (dilution 1:200, Santa Cruz Biotechnology Inc, Santa Cruz, California, sc-1785) followed by incubation with biotin conjugated secondary antibodies. Then the sections were washed and treated with avidin-peroxidase. The sections were developed using the DAB substrate kit (Wako purechemical, Tokyo, Japan) and nuclei were counterstained with hematoxylin. A single observer who was blinded to the experiment protocol performed quantitative analysis. All images were captured with a Nikon microscope equipped with a digital camera (HC-2500) and analyzed by using Adobe Photoshop 6.0 (Adobe Systems, San Jose, California) and Scion Image 1.62 for Windows (Scion, Frederick, Maryland) software. In each case, the average value for 4 to 5 locations or sections for each animal was used for analysis.

Immunofluorescent staining was performed with frozen sections. FITC was stained with anti-FITC antibody (Abcam plc, Cambridge, UK) and nuclei were stained with VECTASHIELD Antifade Mounting Medium with DAPI (Vector Lab, Burlingame, Ca). Fluorescent images were captured by confocal laser microscopy (Olympus FV1000) and analyzed by a single observer as described above.

Near-Infrared Fluorescence Molecular Imaging

Ex vivo fluorescence molecular tomography (FMT) was performed to evaluate macrophage accumulation and matrix metalloproteinase (MMP) activity as previously reported[8, 9]. We used near-infrared fluorescent nanoparticles; Aminospark 680 (Ex/Em=673/690 nm) and MMPSense 750 FAST (Ex/Em=749/775 nm) (PerkinElmer, Inc., Waltham, MA, NEV10142 and NEV10168). These nanoparticles were administered via tail vein 24 hours before imaging. After harvest of the heart and aorta, fluorescent signals from these nanoparticles were captured by dual channel FMT (FMT2000, PerkinElmer, Inc).

Measurements of Statin Tissue Concentration in the Liver and Aorta

For pharmacokinetic analyses, Pitava-NPs (0.1 mg PLGA/ 0.012 mg Pitavastatin/ 200 μl PBS) were intravenously injected. After euthanization at the indicated time points, tissue homogenates were prepared and diluted in methanol. Pitavastatin concentrations in the liver and aorta were determined by high-performance liquid chromatography-tandem mass spectrometry (LC/MS/MS) as follows: separation of the sample was performed on a 150×2 mm, 5 μm analytical column (Develosil C30-UG-5, Nomura Chemical) at 40℃ over 7 minutes with a flow rate of 0.2 mL/min. The high-performance liquid chromatography was next coupled to tandem mass spectrometry by positive turbo ion spray (5500 V).
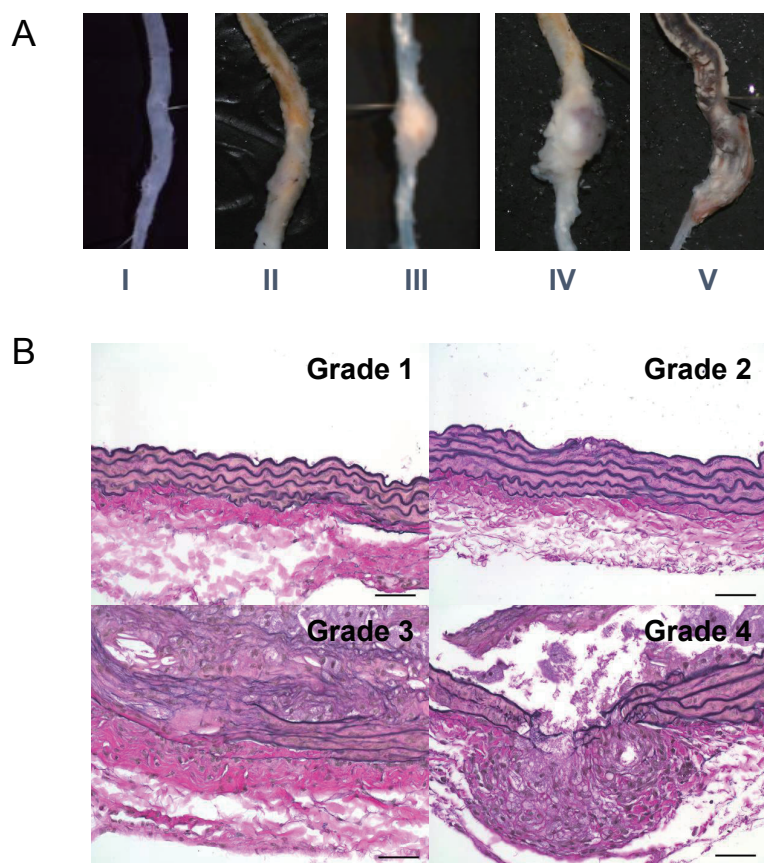
Statistical Analysis

All data are expressed as median±interquartile range. The statistical analysis of differences between two groups was assessed with Mann-Whitney *U*-test, and the statistical analysis of differences among more than two groups was assessed by Kruskal-Wallis test with Dunn's multiple comparison tests. Categorical valuables were assessed by Fisher's exact test. *P* value of

less than 0.05 was considered to be statistically significant.

References

1) Murakami H, Kobayashi M, Takeuchi H and Kawashima Y. Preparation of poly(DL-lactide-co-glycolide) nanoparticles by modified spontaneous emulsification solvent diffusion method. Int J Pharm, 1999; 187: 143-152

2) Kawashima Y, Yamamoto H, Takeuchi H, Hino T and Niwa T. Properties of a peptide containing DL-lactide/glycolide copolymer nanospheres prepared by novel emulsion solvent diffusion methods. Eur J Pharm Biopharm, 1998; 45: 41-48

3) Ishibashi M, Egashira K, Zhao Q, Hiasa K, Ohtani K, Ihara Y, Charo IF, Kura S, Tsuzuki T, Takeshita A and Sunagawa K. Bone marrow-derived monocyte chemoattractant protein-1 receptor CCR2 is critical in angiotensin II-induced acceleration of atherosclerosis and aneurysm formation in hypercholesterolemic mice. Arteriosclerosis, thrombosis, and vascular biology, 2004; 24: e174-178

4) Galimberti D, Fenoglio C, Lovati C, Gatti A, Guidi I, Venturelli E, Cutter GR, Mariani C, Forloni G, Pettenati C, Baron P, Conti G, Bresolin N and Scarpini E. CCR2-64I polymorphism and CCR5Delta32 deletion in patients with Alzheimer's disease. Journal of the neurological sciences, 2004; 225: 79-83

5) Kubo M, Egashira K, Inoue T, Koga J, Oda S, Chen L, Nakano K, Matoba T, Kawashima Y, Hara K, Tsujimoto H, Sueishi K, Tominaga R and Sunagawa K. Therapeutic neovascularization by nanotechnology-mediated cell-selective delivery of pitavastatin into the vascular endothelium. Arteriosclerosis, thrombosis, and vascular biology, 2009; 29: 796-801

6) Daugherty A, Manning MW and Cassis LA. Antagonism of AT2 receptors augments angiotensin II-induced abdominal aortic aneurysms and atherosclerosis. British journal of pharmacology, 2001; 134: 865-870

7) Satoh K, Nigro P, Matoba T, O'Dell MR, Cui Z, Shi X, Mohan A, Yan C, Abe J, Illig KA and Berk BC. Cyclophilin A enhances vascular oxidative stress and the development of angiotensin II-induced aortic aneurysms. Nat Med, 2009; 15: 649-656

8) Koga J, Nakano T, Dahlman JE, Figueiredo JL, Zhang H, Decano J, Khan OF, Niida T, Iwata H, Aster JC, Yagita H, Anderson DG, Ozaki CK and Aikawa M. Macrophage Notch Ligand Delta-Like 4 Promotes Vein Graft Lesion Development: Implications for the Treatment of Vein Graft Failure. Arteriosclerosis, thrombosis, and vascular biology, 2015; 35: 2343-2353

9) Nakashiro S, Matoba T, Umezu R, Koga J, Tokutome M, Katsuki S, Nakano K, Sunagawa K and Egashira K. Pioglitazone-Incorporated Nanoparticles Prevent Plaque Destabilization and Rupture by Regulating Monocyte/Macrophage Differentiation in ApoE(-/-) Mice. Arterioscl Throm Vas, 2016; 36: 491-500

Supplementary Fig. 1.

A, Severity grade of abdominal aortic aneurysm formation. B, Elastin degradation grade of abdominal aortic aneurysm formation.

Supplementary Table 1. Tissue concentration of pitavastatin in the liver in Pitava-NP group

	2 hours (N=3)	6 hours (N=3)	24 hours (N=3)
Concentration (ng/g)	24.3 ± 4.4	5.4 ± 1.5	N.D.

The data are expressed as the mean ± SEM. N.D. indicates not determined (values less than the lower limit of quantification (2.5 ng/g)).

Supplementary Table 2. Tissue concentration of pitavastatin in the aorta in Pitava-NP group

	2 hours (N=3)	6 hours (N=3)	24 hours (N=3)
Concentration (ng/g)	10.7 N.D. (3.6>) N.D. (7.1>)	N.D. (3.6>) N.D. (5.0>) N.D. (5.0>)	9.5 N.D. (2.5>) N.D. (3.6>)

N.D. indicates not determined (values less than the indicated lower limit of quantification).